Electrochemistry Communications 126 (2021) 107018

Contents lists available at ScienceDirect

Electrochemistry Communications

journal homepage: www.elsevier.com/locate/elecom

Polymer pencil leads as a porous nanocomposite graphite material for electrochemical applications: The impact of chemical and thermal treatments

Libuse Trnkova [a,*], Iveta Triskova [a], Jan Cechal [b], Zdenek Farka [c,d]

[a] Department of Chemistry, Faculty of Science, Masaryk University, Kamenice 5, 625 00 Brno, Czech Republic
[b] CEITEC BUT, Brno University of Technology, Purkynova 123, 612 00 Brno, Czech Republic
[c] Department of Biochemistry, Faculty of Science, Masaryk University, Kamenice 5, 625 00 Brno, Czech Republic
[d] CEITEC MU, Masaryk University, Kamenice 5, 625 00 Brno, Czech Republic

ARTICLE INFO

Keywords:
Polymer pencil graphite electrode
Nanocomposite
Microporous electrodes
Siloxanes
Redox processes of chlorides

ABSTRACT

Pencil graphite electrodes are a simple, disposable, and low-cost alternative to screen-printed graphite electrodes. In terms of stability and sensitivity, pencil electrodes often outperform conventional carbon ones. This paper discusses and emphasizes the superior properties of polymer pencil graphite electrodes (pPeGEs), which can be exploited in the electrochemical analysis of molecules, such as chlorides, whose signals are missing on common graphite electrodes. The chemical and structural behaviour of pencil leads after exposure to acids (HF, HNO_3, $HClO_4$) or organic solvents (CH_3CN, CH_3Cl) was monitored *via* X-ray photoelectron spectroscopy (XPS) and scanning electron microscopy (SEM). The electrochemical activity of pristine and treated pPeGEs was studied by the cyclic voltammetry (CV) responses of reversible redox probes $[Fe(CN)_6]^{3-/4-}$ and $[Ru(NH_3)_6]^{3+/2+}$. XPS proved the presence of siloxanes in the surface matrix of the pencil leads; this finding relates to the hydrophobic surface character of the electrodes. SEM then provided images of the pencil surfaces with microplates and flakes and revealed the removal of siloxanes upon chemical treatment. The CVs of non-dried and dried pPeGEs displayed surface changes in the polymer matrix, accompanied by water loss. Our study shows that the pPeGE retains the character of a stable graphite sensor when exposed to acids and organic solvents, except for HF and chloroform. The discovered effects explain the electrochemical processes occurring on pPeGEs and can contribute to their application in electrochemical sensing and energy storage.

1. Introduction

In 1795, Jacques Conte started producing mechanical pencil leads based on graphite powder with clay as the binder [1]. The pure graphite component remains irreplaceable as the most important raw material in pencil manufacturing. However, the composition of the binder is being continuously developed, while maintaining the form of a pencil rod. The production of pencil leads starts by kneading a mixture of graphite, the binder, and water. Afterwards, the mixture is pressed and dried to be eventually fired at high temperatures (between 800 and 1,000 °C). To prevent carbon combustion, the pencil lead must be fired in an oxygen-free atmosphere [2,3]. Changing the ratio between the graphite and the binder affects the pore size, which is connected with the hardness of the lead. The leads are then treated in a preparation bath usually consisting of oils, glycerol, and other components; however, the list of components in the product data sheets is limited [4]. The "polymer" branding of commercial pencil leads is due to the polymeric nature of the surface coating. As the leads are composed of graphite and binder particles, they are considered to be a nanocomposite material, with properties significantly different from those of pure graphite [1,5–7].

As well as their primary use in writing, pencil leads find application in electrochemistry, as an electrode material [8–15]. Polymer pencil graphite electrodes (pPeGEs) have excellent properties [16–20] with respect to their (i) functionality over a wide potential range, (ii) good reproducibility, (iii) high signal-to-noise ratio, (iv) low background current, (v) fast electron transfer, and, in some cases, (vi) portability and (vii) stability [16]. Furthermore, pPeGEs are significantly cheaper (~0.06 €) than screen-printed graphite electrodes (~2.7 €), allowing

* Corresponding author.
E-mail address: libuse@chemi.muni.cz (L. Trnkova).

https://doi.org/10.1016/j.elecom.2021.107018
Received 24 February 2021; Received in revised form 11 March 2021; Accepted 14 March 2021
Available online 23 March 2021

them to be treated as disposable.

Pencil leads are also used to produce graphitic deposits (the pencil trace on a sheet of paper), which can be exploited for electrochemical sensing [21]. Paper has an abrasive impact on pencil lead, leading to exfoliation of the graphitic material and a transfer of the graphene layers to the cellulose fibres. The electrochemical exfoliation of graphene from a pencil core with different graphite and clay ratios has been described recently [17,19,22].

Pencil leads are typically characterized *via* energy-dispersive X-ray (EDX) spectroscopy, X-ray photoelectron spectroscopy (XPS), Raman spectroscopy, and scanning electron microscopy (SEM) [17,19]. To determine the electrochemical properties, cyclic voltammetry (CV) with redox probes such as $[Fe(CN)_6]^{3-/4-}$, $[Ru(NH_3)_6]^{3+/2+}$ or dopamine is used [16–19]. Their high conductivity and the possibility of resisting surface contamination has facilitated the use of pPeGEs in the fabrication of scanning tunnelling microscopy (STM) tips [23]. Detection setups utilizing pPeGEs in microfluidic or chromatography (HPLC) systems have also recently been characterized [24,25].

Our electroanalytical and mechanistic studies of the oxidation processes of purine derivatives have shown that pPeGEs can provide a more sensitive response than other graphite electrodes (GCE, HOPG). This enhancement was attributed to the accumulation of oxo- and aminopurines on the electrode surface. The elimination voltammetric procedure (EVLS) provided easily read, sharp peak–counterpeak signals of adsorbed electroactive species and allowed us to reach the limits of detection in the nanomolar range [26–31].

The electrochemical activity of pPeGEs is influenced by their mechanical and chemical properties, such as roughness, porosity, mechanical stability, hardness, and surface charge. Therefore, chemical modification of the surface layers, modifications of the pore size, or changes in the surface morphology can help us to understand the mechanism of the sensor and to enhance its sensitivity, including the separation of overlapping signals.

In this paper, we explore the impact of the chemical and thermal treatments of pPeGEs on their electrochemical properties. We investigated (i) the structure and composition of the surfaces upon exposure to strong inorganic acids or organic solvents, (ii) the effect of both chemical and thermal treatment on the electron transfer kinetics, and (iii) their sensitivity to chlorides. The pPeGEs were treated and examined using three methods: CV, XPS, and SEM. Our study shows that the pPeGE is a porous nanocomposite graphite electrode with unique behaviour towards water and the ions present in the solution.

2. Experimental

2.1. Chemicals and materials

Commercially available pencil leads (Ultra-polymer, 0.5 HB) were purchased from Tombow (Japan). The chemicals for the calibration redox systems included $K_3[Fe(CN)_6]$ and $K_4[Fe(CN)_6]$ (Lachema, p.a.), $Ru[(NH_3)_6]Cl_3$ (Sigma-Aldrich, p.a.), and KCl (Sigma-Aldrich, ACS grade). The electrode treatment was carried out with HF (48% in H_2O; ≥99.99%), HNO_3 (65%; p.a.), $HClO_4$ (70%; p.a.), acetonitrile (for HPLC, gradient grade), or chloroform (p.a.) purchased from Sigma-Aldrich, Merck, or Penta, without further purification. All of the solutions were prepared in deionized Milli-Q water (18.2 MΩ·cm at 25 °C).

2.2. Preparation of the chemically treated pPeGEs

The pencil leads were immersed in solutions of concentrated acids (HF, HNO_3, $HClO_4$) or organic solvents (acetonitrile, chloroform) and soaked for 24 h. After the treatment, the leads were washed with Milli-Q water (thrice for 20 min with shaking). The leads treated with acetonitrile or chloroform were air-dried at 25 °C for 1 h.

2.3. X-ray photoelectron spectroscopy (XPS)

XPS was performed on an Axis-Ultra DLD (Kratos, UK) system, using monochromatic Al-Kα radiation, with the magnetic lens turned on. No charge compensation was necessary, as proper grounding of the samples was ensured. The pencil leads were placed over an opening in the sample plate to exclude the potential contribution of a substrate signal. Pass energies of 160 eV and 20 eV were employed in the survey and the detailed spectra, respectively. The quantification was carried out using the ESCAPE software, utilizing instrument-related sensitivity factors.

2.4. Scanning electron microscopy (SEM)

A SEM Versa 3D (FEI, USA) was used to characterize the morphologies of the pPeGEs before and after chemical treatment. A conductive tape facilitated fixing of the electrodes and prevented charging effects during scanning. The measurement was performed at 5 kV in secondary electron mode with an Everhart-Thornley detector.

2.5. Cyclic voltammetry (CV)

The voltammetric experiments were performed using a μAutolab Type III electrochemical analyser (Metrohm, Switzerland) with the GPES Manager 4.9 software. The voltammetric cell was equipped with three electrodes: a pPeGE as the working electrode (dipped 10 mm deep in the solution); an Ag/AgCl/3 M KCl electrode as the reference; and a Pt wire as the auxiliary electrode. A pencil lead was inserted into a tube holder with a gold tubular FRB Tesla connector. The electrical contact was achieved by soldering a copper wire to the gold connector. The immersion depth of the pPeGE (10 mm) was checked by means of an attached scale. The reproducibility of our measurements corresponds to a RSD ≤ 3.5% measured by CV.

The pPeGEs were characterized *via* CV with redox probes of 1 mM $[Fe(CN)_6]^{3-/4-}$ (the potential range was − 0.3 V to 0.8 V) or 1 mM $[Ru(NH_3)_6]^{3+/2+}$ (−0.4 V to 0.2 V) in 0.1 M KCl. The scan rates ranged from 100 to 800 mV/s; the potential step corresponded to 2 mV. The CV curves of the chlorides were measured in the potential range from − 0.1 V to 1.8 V using scan rates between 25 and 200 mV/s and a potential step of 2 mV. All of the experiments were carried out at room temperature.

The effective area of the pPeGEs, A_{eff}, was calculated according to the Randles–Sevcik equation [32]:

$$A_{eff} = I_p / \left(2.69 \cdot 10^5 \cdot n^{3/2} \cdot D^{1/2} \cdot c \cdot v^{1/2}\right) \quad (1)$$

where A_{eff} is the electrode area (cm^2); I_p denotes the peak current (A); n represents the number of electrons transferred in the redox process; D is the diffusion coefficient ($cm^2 \cdot s^{-1}$); c stands for the concentration ($mol \cdot cm^{-3}$); and v denotes the scan rate ($V \cdot s^{-1}$). The diffusion coefficients of $[Fe(CN)_6]^{3-/4-}$ and $[Ru(NH_3)_6]^{3+/2+}$ in 0.1 M KCl are $7.62 \cdot 10^{-6}$ $cm^2 \cdot s^{-1}$ and $8.43 \cdot 10^{-6}$ $cm^2 \cdot s^{-1}$, respectively [33,34].

3. Results and discussion

3.1. X-ray photoelectron spectroscopy (XPS) characterization of the pPeGEs

The elemental composition of the pPeGEs was determined *via* XPS before and after chemical treatment. The survey XPS spectra for the pristine and chloroform-treated pencil leads are shown in Fig. 1A. The quantitative analysis revealed that the pristine pPeGE comprised 80.0% carbon, 9.5% oxygen, and 10.5% silicon atoms. A detailed evaluation of the individual peaks and their components (see Supplementary Information) showed that the majority of the carbon is in the form of graphite [35]. The two minor components were associated with the sp^3 carbon in the aliphatic hydrocarbons (285.0 eV) [36] and Si–C bonds (284 eV). Both the position and the intensities of the O 1s and Si 2p peaks were consistent with the $[–Si–O–Si–O–]_n$ structure of siloxanes [37]. This

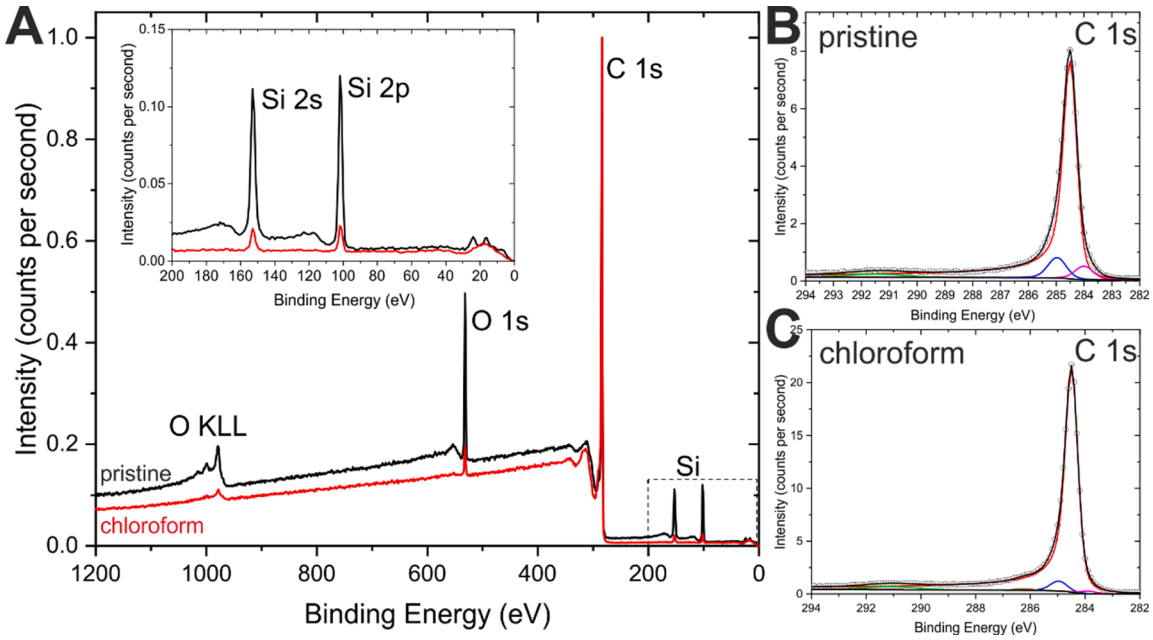

Fig. 1. (A) The survey XPS spectra of the pristine (black) and the chloroform-treated (red) pPeGEs; the inset shows a magnified view of the Si peaks enclosed by the dashed rectangle. The detailed C 1s spectra of (B) pristine and (C) chloroform-treated pPeGEs. (For interpretation of the references to colour in this figure legend, the reader is referred to the web version of this article.)

siloxane-related polymer was present mainly near the surface of the pencil leads, as discussed in the Supplementary Information.

When the pencil was scraped with a scalpel to half of its diameter, the composition of the core significantly differed from that of the surface, comprising 96.5% carbon, 2.5% oxygen, and 1% silicon. The XPS results before and after chemical treatment of the pPeGEs are summarized in Table 1. The atomic concentrations of C, O, and Si are given with standard deviations up to 2%; on some acid-treated samples, trace amounts of Cl- and N-associated peaks were measured near the detection limit (the associated concentrations would be below 1%). Note that in the case of the HF and $HClO_4$ treatments, the results fall into two categories as marked within the table; this discrepancy is consistent with limited reproducibility of the electrochemical response. In all of the other samples, the results were reproducible.

The quantitative analysis showed relatively small XPS spectral differences between the pristine and the treated pencil leads, except for the modification in chloroform. This was confirmed not only by the values in Table 1, approaching the intensities of the scraped lead (bulk), but also the significant reduction in the Si peaks in the survey spectrum (Fig. 1A).

Table 1
The results of the quantitative analysis of the XPS spectra of the pPeGEs. The first three columns give the atomic concentrations of C, O, and Si, respectively; the fourth column shows the ratio of the oxygen and silicon concentrations; the remaining columns provide relative fractions of the C 1s peak components based on peak fitting.

pPeGE					C 1s peak		
	C	O	Si	O/Si	285.0 eV (sp^3)	284.45 eV (sp^2)	284.0 eV (Si-C)
Pristine							
Surface	80.0	9.5	10.5	0.9	7.3	87.9	4.8
Bulk	96.5	2.5	1.0	2.5	1.1	97.7	1.2
Treated							
HNO_3	85.0	7.8	7.2	1.08	3.0	92.7	4.3
$HClO_4$ (1)	88.0	7.1	4.9	1.45	5.0	90.4	4.6
$HClO_4$ (2)	75.5	12.4	12.1	1.03	5.1	82.0	12.9
HF (1)	70.5	15.3	14.2	1.08	5.9	79.7	14.4
HF (2)	76.0	12.5	11.5	1.08	5.6	88.9	5.5
Acetonitrile	84.6	7.5	7.9	0.94	6.7	88.7	4.6
Chloroform	96.5	1.9	1.6	1.25	3.6	95.4	1.0

3.2. *Scanning electron microscopy (SEM) characterization of the pPeGEs*

SEM was employed to probe the surface morphologies and microstructures of the pPeGEs before and after various types of chemical treatment (Fig. 2). At the magnification of 50,000×, graphite flakes were discerned on the surfaces of both the pristine and the modified electrodes. As regards the acids (HNO_3, $HClO_4$, and HF), the treatment resulted in a more structured surface, with typical features in the size

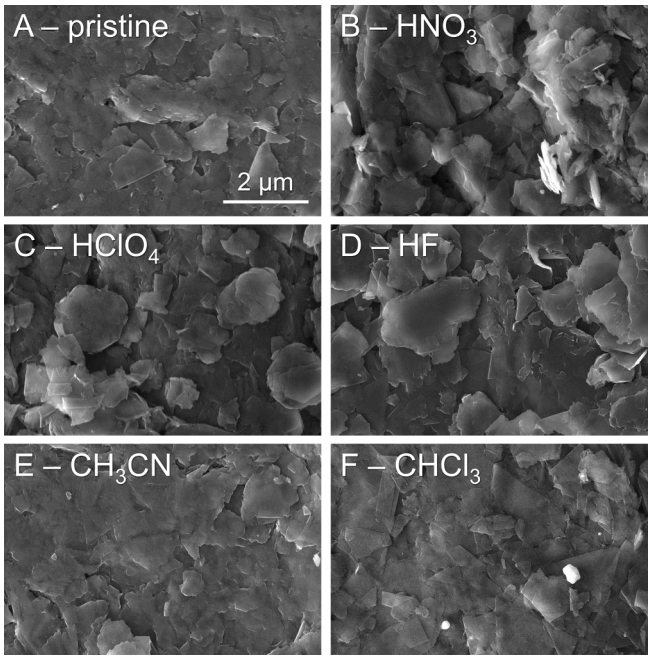

Fig. 2. SEM images of the (A) pristine pPeGE and the pPeGEs after treatment in (B) HNO_3, (C) $HClO_4$, (D) HF, (E) acetonitrile, and (F) chloroform.

range 0.5 to 3 μm. Furthermore, these main features exhibited nanometer-sized wrinkles. These results suggest a higher value for the effective electroactive surface of the electrodes. In the treatment with organic solvents (CH_3CN and $CHCl_3$), the morphology changes were not as significant as those after the acid cycle.

3.3. Cyclic voltammetry (CV) characterization of the pPeGEs

The electrochemical characterization of the electrode systems was delivered by using the well-known anionic $[Fe(CN)_6]^{3-/4-}$ and cationic $[Ru(NH_3)_6]^{3+/2+}$ redox probes [18,38]. These redox pairs differ in their charges, leading to distinct behaviour on graphite surfaces. The ruthenium complex is relatively insensitive to the graphite surface state, and its electron transfer takes place *via* electron tunnelling, even through an adsorbed layer of organic substances. Conversely, the ferro/ferricyanide complex exhibits specific surface interactions and is, therefore, more sensitive to changes in the electrode surface [18]. The interactions, together with the electron transfer (ET) of the redox pairs at the molecular level, are manifested macroscopically in the voltammetric peak separation values (ΔE_p); larger ΔE_p values indicate a slower rate of electron transfer, and *vice versa*.

Table 2
The CV-based characterization of the pPeGEs before and after chemical treatment (scan rate: 200 mV/s).

pPeGE	$[Fe(CN)_6]^{3-/4-}$		$[Ru(NH_3)_6]^{3+/2+}$	
	ΔE_p (mV)	A_{eff} (cm^2)	ΔE_p (mV)	A_{eff} (cm^2)
Pristine	75 ± 2	0.110 ± 0.012	75 ± 2	0.080 ± 0.010
Treated				
HNO_3	84 ± 2	0.120 ± 0.019	85 ± 2	0.108 ± 0.017
$HClO_4$	79 ± 3	0.119 ± 0.014	73 ± 3	0.087 ± 0.015
HF	97 ± 5	0.112 ± 0.012	73 ± 3	0.078 ± 0.020
acetonitrile	80 ± 2	0.115 ± 0.011	74 ± 1	0.061 ± 0.011
chloroform	125 ± 5	0.136 ± 0.014	73 ± 2	0.052 ± 0.012

The ΔE_p and the A_{eff} were determined as the average of the values obtained for 5–7 electrodes.

The height of the voltammetric peaks (I_p) at a known concentration c and diffusion coefficient D provides the effective electrode area A_{eff} (Eq. (1)).

Both the pristine and the chemically treated pPeGEs were tested by using the above-mentioned redox probes; the ΔE_p and A_{eff} values are summarized in Table 2. The pristine pPeGE provided the same ΔE_p values for $[Fe(CN)_6]^{3-/4-}$ and $[Ru(NH_3)_6]^{3+/2+}$ probes, indicating identical ET kinetics. In the case of the ruthenium complex, no significant changes in the ΔE_p were observed upon chemical treatment; the only exception was HNO_3, which resulted in an increased ΔE_p. By contrast, the results obtained for the ferro/ferricyanide complex showed significant fluctuations in the ΔE_p after treatment, an effect related to interactions with the changing electrode surface. Surprisingly, the changes in the A_{eff} showed an opposite trend. With the ferro/ferricyanide complex, the value of A_{eff} remained relatively constant after the various treatments (variation within ~ 15%). The greatest increment was observed in chloroform, indicating its attack on the pPeGE surface; this finding is in agreement with that obtained *via* XPS. Conversely, the Ru complex exhibited differences in the value of A_{eff} after various treatments, and the values were generally lower (about 20–50%) than those acquired with the ferro/ferri complex. In this case, too, the largest difference occurred after the chloroform treatment; however, a decrease was observed, unlike the situation with the ferro/ferricyanide probe, where the chloroform produced an increased A_{eff}. Overall, we can claim that the $[Fe(CN)_6]^{3-/4-}$ probe provides larger ΔE_p changes and smaller A_{eff} variations than the $[Ru(NH_3)_6]^{3+/2+}$ probe. These findings are consistent with the XPS results (Table 1).

After the acid treatment, the electrodes were washed with water and dried, causing lower reproducibility of the CV parameters. A closer look at the drying procedure revealed that these changes are connected with variations in the drying time. This directed us towards studying the effect of temperature-dependent changes in the surface siloxanes and the role of water, which could enter the porous material of the electrode. Thus, we performed experiments where non-dried and dried (200 °C, 24 h) pPeGEs were examined using the $[Fe(CN)_6]^{3-/4-}$ probe. The CV curves and the relevant data are shown in Fig. 3 and Table 3, respectively.

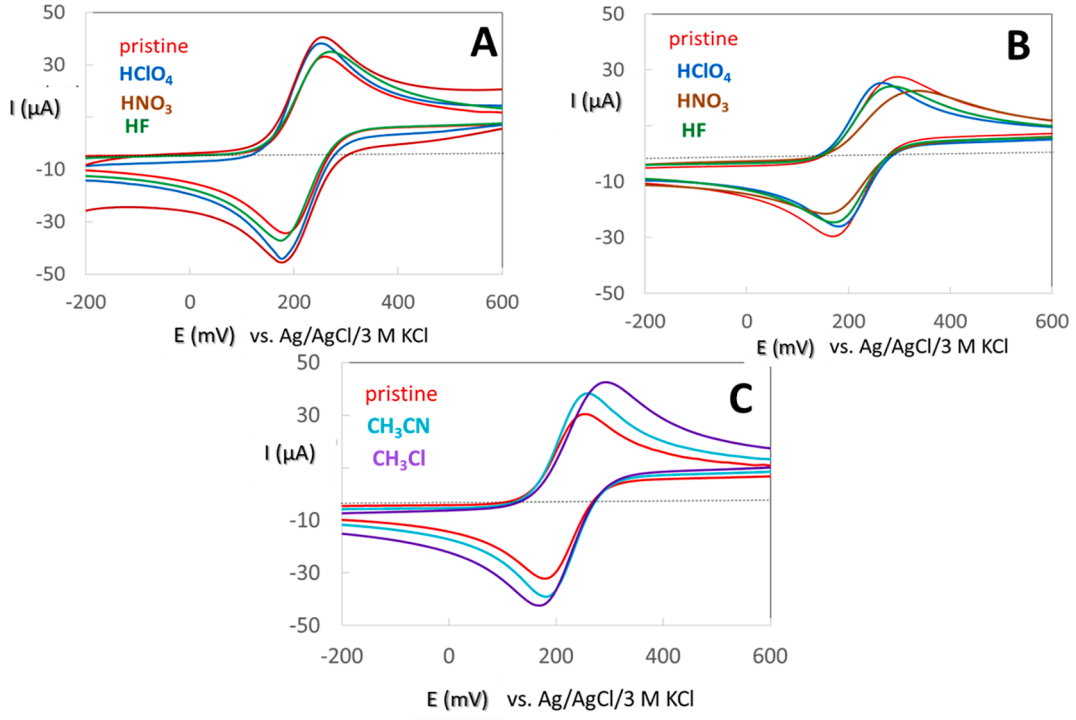

Fig. 3. The cyclic voltammograms of the pristine and the treated pPeGEs in 1 mM $[Fe(CN)_6]^{3-/4-}$ in 0.1 M KCl (the scan rate of 200 mV/s). The CV curves for the pristine pPeGEs and after treatment with $HClO_4$, HNO_3, and HF; (A) without drying, and (B) after drying at 200 °C for 24 h. (C) The CV curves of the pristine pPeGEs and after acetonitrile and chloroform-based treatments (without drying).

Table 3
The impact of surface water on the CV parameters of the pPeGEs.

pPeGE	$[Fe(CN)_6]^{3-/4-}$ non-dried		$[Fe(CN)_6]^{3-/4-}$ dried	
	ΔE_p (mV)	A_{eff} (cm^2)	ΔE_p (mV)	A_{eff} (cm^2)
Pristine	75 ± 2	0.110 ± 0.012	129 ± 2	0.080 ± 0.014
Treated				
HNO_3	84 ± 2	0.120 ± 0.018	179 ± 2	0.069 ± 0.015
$HClO_4$	79 ± 3	0.119 ± 0.013	83 ± 5	0.080 ± 0.017
HF	97 ± 5	0.112 ± 0.019	113 ± 44	0.072 ± 0.012

The effect of the drying and heat treatment of the pencil leads on the ferro/ferri ET is displayed in Fig. 4. The largest changes in the ΔE_p and the A_{eff} were observed in nitric acid. The strong impact of the heat treatment on the electrochemical behaviour of the pPeGEs was supported not only by the CV (Table 3) but also by the electrical conductivity value. In the non-dried electrode, the electrical conductivity was almost double (732 S/m) that of the dried one (429 S/m). We can assume that the thermal properties of the surface poly(siloxanes) were changed [39], and water was removed from the pores of the pPeGE. The CV of the ferro/ferri probe measured at 200 mV/s revealed that the largest difference between the dried and the non-dried pencil leads was observed for HNO_3, where water caused a difference in the ΔE_p of almost 100 mV (Fig. 4).

3.4. Redox processes of chlorides on the pPeGEs

The anodic polarization of the pristine pPeGE to potentials greater than 1.2 V (vs. Ag/AgCl/3 M KCl) in 0.1 M KCl indicated voltammetric oxidation waves of the chlorides in the anodic and a reduction of the chlorine in the cathodic parts of the cyclic voltammogram (Fig. 5). The chloride signals recorded by us agree with the standard redox potential of chlorides (1.396 V vs. NHE) and also with the results of previous publications [40–42]. The impact exerted by the chemical treatment of the electrodes on the response of the chlorides is compared in Fig. 5B and C). The CV records of the chlorides showed that the most significant effect was observed in the case of chloroform (Fig. 5C, violet), which corresponds to the above-mentioned results. The linear dependence of the wave or peak heights on the square root of the scan rate indicated that both the oxidation of the Cl^- and the reduction of the Cl_2 are diffusion-controlled (not shown).

The pencil surface is intensively structured, with many microplates and flakes; their edges create areas of high charge density allowing high charge-transfer rates. Therefore, the pPeGEs can catalyse electrode processes with sluggish kinetics. For example, consider the above-mentioned redox behaviour of the chlorides, which are poorly detectable on GCEs (Fig. S2). The effect of pore water was also reflected in the redox process of chlorides, as illustrated in Fig. S3.

Our results also revealed that the pPeGEs have a high conductivity

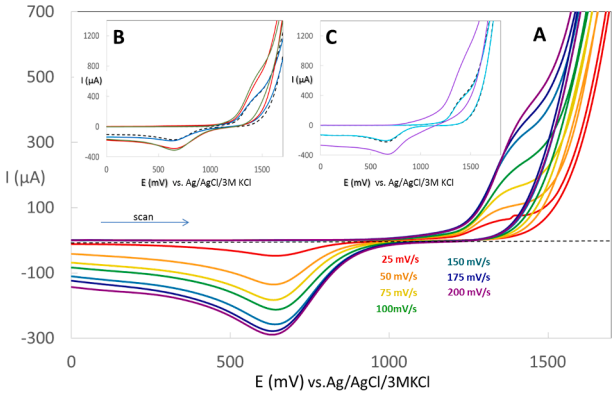

Fig. 5. (A) The cyclic voltammograms of the chlorides (0.1 M KCl in 0.1 mM HNO_3) recorded at different scan rates (from 25 mV/s to 200 mV/s) on the pristine pPeGE and after treatment with (B) acids and (C) organic solvents (scan rate 200 mV/s).

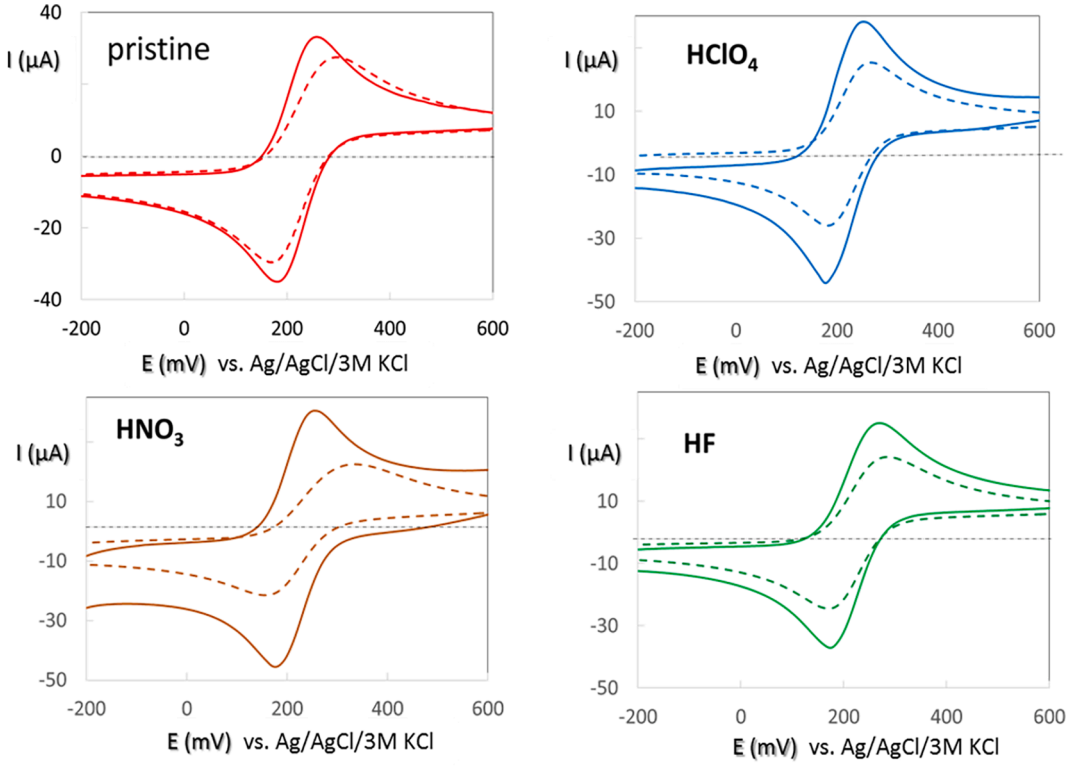

Fig. 4. A comparison of the cyclic voltammograms of the non-dried (full lines) and the dried pPeGEs (dashed lines), pristine and chemically treated. The scan rate was 200 mV/s.

and an abundance of slit-like pores that can retain water. Thus, water is present, even though the surface of the pPeGEs is hydrophobic due to the presence of (poly)siloxanes. The Si is bond-saturated by oxygen in the siloxane structure; however, the oxygen may play the role of a Lewis base, offering the possibility of binding not only the cations and protonated small organic molecules but also the water in the form of positively charged clusters. In this manner, the pPeGE surface can accelerate electron transfer processes.

4. Conclusion

We exposed and demonstrated the unique electrochemical properties of pPeGEs relating to their chemical stability and changes upon heat treatment. The electrodes were shown to be composed of a nanocomposite conductive material with a hydrophobic character and a porous structure. In this context, we experimentally verified the presence of polysiloxanes in the pencil lead. The investigation *via* different chemical treatment methods (inorganic acids and organic solvents), eliminating chemicals that dissolve polysiloxanes, revealed the relatively high chemical stability of the pPeGEs. Furthermore, we compared for the first time non-dried and dried pPeGEs, indicating that humidity improves the functioning of the electrodes. To remove the water, we heated the electrodes for 24 h. In the presence of humid air, however, water molecules were observed to fill the pores of the pPeGEs; this process is slow, lasting several hours. Generally, siloxanes, due to their hydrophobicity and chemical composition, may aid the penetration of water into the pores. The water then facilitates the electron transfer, which produces higher electrical conductivity and lower background currents. These effects were highlighted by the electroanalysis of the chlorides: detection was feasible only in the pPeGEs whose pores contained water, although small chloride signals were observed in the dried pPeGEs and conventional carbon electrodes. The presented characterization of pPeGEs leads towards not only a deeper understanding of the electrochemical processes occurring but also the development of advanced electrochemical applications, including sensors and batteries.

CRediT authorship contribution statement

Libuse Trnkova: Conceptualization, Methodology, Visualization, Writing. **Iveta Triskova:** Electrochemical data curation, Visualization. **Jan Cechal:** XPS experiments, Evaluation, **Zdenek Farka:** SEM experiments, Editing.

Declaration of competing interest

The authors declare no competing financial interests or personal relationships that may have influenced the work reported herein.

Acknowledgements

The research was supported by Masaryk University (MUNI/A/1424/2019) Czech Republic and the International Visegrad Fund (22020140). We acknowledge CF Cryo-electron Microscopy and Tomography of CIISB, the Instruct-CZ Centre, supported by MEYS CR (LM2018127). Part of the work was carried out utilizing the infrastructure of Czech-NanoLab supported by MEYS CR (LM2018110). We thank Dr. Vít Vykoukal for taking the SEM images and Mikita Bandarenka for technical help.

Appendix A. Supplementary data

Supplementary data to this article can be found online at https://doi.org/10.1016/j.elecom.2021.107018.

References

[1] F.L. Encke, Chemistry and manufacturing of lead pencil, J. Chem. Educ. 47 (1970) 575–576, https://doi.org/10.1021/ed047p575.
[2] M. Bard, H.-G. Baumgart, US Patent number 4,758,540 (1987).
[3] W. Handl, J.S. Staedtler, US Patent number 5,118,345, (1992).
[4] Staedtler, http://www.officestationery.co.uk/documents/113733.pdf, (2016).
[5] R.N. Bhowmik, Ferromagnetism in lead graphite-pencils and magnetic composite with $CoFe_2O_4$ particles, Compos. B Eng. 43 (2) (2012) 503–509, https://doi.org/10.1016/j.compositesb.2011.07.013.
[6] J.A. Denman, I.M. Kempson, W.M. Skinner, K.P. Kirkbride, Discrimination of pencil markings on paper using elemental analysis: an initial investigation, Forensic Sci. Int. 175 (2-3) (2008) 123–129, https://doi.org/10.1016/j.forsciint.2007.05.017.
[7] M.S. Dresselhaus, G. Dresselhaus, Intercalation compounds of graphite, Adv. Phys. 51 (1) (2002) 1–186, https://doi.org/10.1080/00018730110113644.
[8] M.R. Akanda, M. Sohail, M.A. Aziz, A.-N. Kawde, Recent advances in nanomaterial-modified pencil graphite electrodes for electroanalysis, Electroanalysis 28 (3) (2016) 408–424, https://doi.org/10.1002/elan.201500374.
[9] I.G. David, D.-E. Popa, M. Buleandra, Pencil graphite electrodes: a versatile tool in electroanalysis, J. Anal. Methods Chem. 2017 (2017) 1–22, https://doi.org/10.1155/2017/1905968.
[10] A. Erdem, E.S. Urkac, H. Karadeniz, A. Caliskan, E. Oks, A. Nikolayev, A. Oztarhan, Electrochemical behavior of disposable electrodes prepared by ion beam based surface modification for biomolecular recognition, in: F.D. McDaniel, B.L. Doyle (Eds.) Application of Accelerators in Research and Industry, vol. 1099, 2009, pp. 531–534.
[11] M. Findik, H. Bingol, A. Erdem, Hybrid nanoflowers modified pencil graphite electrodes developed for electrochemical monitoring of interaction between Mitomycin C and DNA, Talanta 222 (2021) 121647, https://doi.org/10.1016/j.talanta.2020.121647.
[12] P. Kara, A. Erdem, S. Girousi, M. Ozsoz, Electrochemical detection of enzyme labeled DNA based on disposable pencil graphite electrode, J. Pharm. Biomed. Anal. 38 (1) (2005) 191–195, https://doi.org/10.1016/j.jpba.2004.12.011.
[13] A.-N. Kawde, N. Baig, M. Sajid, Graphite pencil electrodes as electrochemical sensors for environmental analysis: a review of features, developments, and applications, RSC Adv. 6 (94) (2016) 91325–91340, https://doi.org/10.1039/C6RA17466C.
[14] S.A. Ozkan, B. Uslu, From mercury to nanosensors: past, present and the future perspective of electrochemistry in pharmaceutical and biomedical analysis, J. Pharm. Biomed. Analysis 130 (2016) 126–140, https://doi.org/10.1016/j.jpba.2016.05.006.
[15] A. Torrinha, C.G. Amorim, M. Montenegro, A.N. Araujo, Biosensing based on pencil graphite electrodes, Talanta 190 (2018) 235–247, https://doi.org/10.1016/j.talanta.2018.07.086.
[16] K. Aoki, T. Okamoto, H. Kaneko, K. Nozaki, A. Negishi, Applicability of graphite reinforcement carbon used as the lead of a mechanical pencil to voltammetric electrodes, J. Electroanal. Chem. 263 (2) (1989) 323–331, https://doi.org/10.1016/0022-0728(89)85102-2.
[17] J.K. Kariuki, An electrochemical and spectroscopic characterization of pencil graphite electrodes, J. Electrochem. Soc. 159 (9) (2012) H747–H751.
[18] R.L. McCreery, Advanced carbon electrode materials for molecular electrochemistry, Chem. Rev. 108 (7) (2008) 2646–2687, https://doi.org/10.1021/cr068076m.
[19] R. Navratil, A. Kotzianova, V. Halouzka, T. Opletal, I. Triskova, L. Trnkova, J. Hrbac, Polymer lead pencil graphite as electrode material: Voltammetric, XPS and Raman study, J. Electroanal. Chem. 783 (2016) 152–160, https://doi.org/10.1016/j.jelechem.2016.11.030.
[20] A. Özcan, Y. Şahin, Preparation of selective and sensitive electrochemically treated pencil graphite electrodes for the determination of uric acid in urine and blood serum, Biosens. Bioelectron. 25 (11) (2010) 2497–2502, https://doi.org/10.1016/j.bios.2010.04.020.
[21] C.W. Foster, D.A.C. Brownson, A.P.R. de Souza, E. Bernalte, J. Iniesta, M. Bertotti, C.E. Banks, Pencil it in: pencil drawn electrochemical sensing platforms, Analyst 141 (2016) 4055–4064.
[22] K.F. Chen, D.F. Xue, S. Komarneni, Nanoclay assisted electrochemical exfoliation of pencil core to high conductive graphene thin-film electrode, J. Colloid Interf. Sci. 487 (2017) 156–161, https://doi.org/10.1016/j.jcis.2016.10.028.
[23] A. Knapek, D. Sobola, D. Burda, A. Danhel, M. Mousa, V. Kolarik, Polymer graphite pencil lead as a cheap alternative for classic conductive SPM probes, Nanomaterials 9 (2019) 1756, https://doi.org/10.3390/nano9121756.
[24] E.W. Nery, M. Kundys-Siedlecka, Y. Furuya, M. Jonsson-Niedziolka, Pencil lead as a material for microfluidic 3D-electrode assemblies, Sensors 18 (2018) 4037, https://doi.org/10.3390/s18114037.
[25] D. Riman, M.I. Prodromidis, D. Jirovsky, J. Hrbac, Low-cost pencil graphite-based electrochemical detector for HPLC with near-coulometric efficiency, Sensor Actuat. B: Chem. 296 (2019) 126618, https://doi.org/10.1016/j.snb.2019.05.095.
[26] N. Aladag, L. Trnkova, A. Kourilova, M. Ozsoz, F. Jelen, Voltammetric study of aminopurines on pencil graphite electrode in the presence of copper ions, Electroanalysis 22 (15) (2010) 1675–1681, https://doi.org/10.1002/elan.v22:1510.1002/elan.201000031.
[27] R. Navratil, F. Jelen, Y. Ugur, Kayran, L. Trnkova, A pencil graphite electrode in situ modified by monovalent copper: a promising tool for the determination of methylxanthines, Electroanalysis 26 (5) (2014) 952–961, https://doi.org/10.1002/elan.v26.510.1002/elan.201400017.

[28] R. Navratil, I. Pilarova, F. Jelen, L. Trnkova, Comparative voltammetric analysis of adenine and xanthine on a pencil graphite electrode in the presence of copper ions, Int. J. Electrochem. Sci. 8 (2013) 4397–4408.
[29] N. Serrano, A. Alberich, L. Trnkova, Oxidation of 6-benzylaminopurine-copper(I) complex on pencil graphite electrode, Electroanalysis 24 (2012) 955–960, https://doi.org/10.1002/elan.201100702.
[30] V.K. Sharma, F. Jelen, L. Trnkova, Functionalized solid electrodes for electrochemical biosensing of purine nucleobases and their analogues: a review, Sensors 15 (2015) 1564–1600, https://doi.org/10.3390/s150101564.
[31] V.K. Sharma, L. Trnkova, Copper nanoparticle modified pencil graphite electrode for electroanalysis of adenine, Electroanalysis 28 (11) (2016) 2834–2840, https://doi.org/10.1002/elan.201600237.
[32] A.J. Bard, L.R. Faulkner, Electrochemical Methods: Fundamentals and Applications, second ed., John Wiley and Sons, USA, 2001.
[33] S.J. Konopka, B. McDuffie, Diffusion coefficients of ferricyanide and ferrocyanide ions in aqueous media using twin-electrode thin-layer electrochemistry, Anal. Chem. 42 (1970) 1741–1746, https://doi.org/10.1021/ac50160a042.
[34] Y. Wang, J.G. Limon-Petersen, R.G. Compton, Measurement of the diffusion coefficients of $Ru(NH_3)(6)$ (3+) and $Ru(NH_3)(6)$ (2+) in aqueous solution using microelectrode double potential step chronoamperometry, J. Electroanal. Chem. 652 (1-2) (2011) 13–17, https://doi.org/10.1016/j.jelechem.2010.12.011.
[35] J.A. Leiro, M.H. Heinonen, T. Laiho, I.G. Batirev, Core-level XPS spectra of fullerene, highly oriented pyrolitic graphite, and glassy carbon, J. Electron Spectrosc. 128 (2-3) (2003) 205–213, https://doi.org/10.1016/S0368-2048(02)00284-0.
[36] J. Cechal, T. Sikola, Flexible foils formed by a prolonged electron beam irradiation in scanning electron microscope, Appl. Surf. Sci. 423 (2017) 538–541, https://doi.org/10.1016/j.apsusc.2017.06.236.
[37] P. Louette, F. Bodino, J.-J. Pireaux, Poly(dimethyl siloxane)(PDMS) XPS reference core level and energy loss spectra, Surf. Sci. Spectra 12 (1) (2005) 38–43, https://doi.org/10.1116/11.20050908.
[38] R.G. Compton, C.E. Banks, Understanding Voltammetry, Imperial College Press, 2011.
[39] P.R. Dvornic, Thermal properties of polysiloxanes, in: R.G. Jones, W. Ando, J. Chojnowski (Eds.), Silicon-Containing Polymers, Ch. 7, Springer, Netherlands, 2000, pp. 182–212.
[40] G. Dryhurst, P.J. Elving, Electrooxidation of halides at pyrolytic graphite electrode in aqueous and acetonitrile solutions, Anal. Chem. 39 (6) (1967) 606–615, https://doi.org/10.1021/ac60250a014.
[41] E.R. Lowe, C.E. Banks, R.G. Compton, Gas sensing using edge-plane pyrolytic-graphite electrodes: electrochemical reduction of chlorine, Anal. Bioanal. Chem. 382 (4) (2005) 1169–1174, https://doi.org/10.1007/s00216-005-3223-3.
[42] E. Lowe, C. Banks, R. Compton, Edge plane pyrolytic graphite electrodes for halide detection in aqueous solutions, Electroanalysis 17 (18) (2005) 1627–1634, https://doi.org/10.1002/(ISSN)1521-410910.1002/elan.v17:1810.1002/elan.200503267.